

# Object Contour Matching Using the Biorthogonal Wavelet Transform

Xiaojun Qi

Computer Science Department, Utah State University

4205 Old Main Hill, Logan, UT 84322

[Xiaojun.Qi@usu.edu](mailto:Xiaojun.Qi@usu.edu)

## Abstract

Object contour matching is essential in content-based indexing and retrieval of digital images. In this paper, an automated biorthogonal-wavelet-transform-based object contour matching method is proposed. First, a wavelet transform modulus maxima (WTMM) image is produced by a one level biorthogonal wavelet transform. This WTMM image contains curvature points of the contour. Then the high curvature points (HCPs) are kept in the WTMM image whereas the less important points are discarded. These HCPs are further utilized to locate the centroid of the object contour. Finally, a feature vector for matching object contour is constructed by the sorted distances between each HCP and the centroid. This feature vector is invariant to the translation, rotation, and scale changes. The experimental results demonstrate that the proposed approach can accurately and efficiently match the object contour under these three changes.

**Keywords:** object contour, high curvature points, biorthogonal wavelet transform, wavelet transform modulus maxima, and feature vector.

## 1. Introduction

Content-based indexing and retrieval (CBIR) of digital images has become an active research area since the early 1990s. Most of these CBIR systems support the following one or several functionalities: browse, search by example, and search by a single or a combination of low level features (e.g., color, contour, texture, and spatial layout of objects) extracted from the image.

Hoffman et al. [1] demonstrate that the human visual system decomposes objects at high curvature points (HCPs). These HCPs can be connected via straight lines to approximate curves and retain the maximal amount of information necessary for successful contour recognition. Teh and Chin [2] prove that HCP-based features are robust for recognizing objects due to their invariance to the translation, rotation, and scale changes. Russ [3] applies the corner-based representation of objects to reduce the feature vector size. Han and Jiang [4] propose an HCP-based approach to provide reliable clues about the objects under partial occlusion and

varying background levels. Cheikh et. al. [5] present a wavelet-based shape recognition algorithm to construct two feature vectors from the wavelet transform modulus maxima (WTMM) of the object contour at each dyadic scale from  $2^1$  to  $2^6$ . These two feature vectors contain the important HCPs and their locations. Khalil et. al [6] study the object recognition invariant functions calculated by different dyadic scales of wavelet transform. Belongie et. al. [7] propose a shape-context-based approach to measuring similarity between shapes and exploit it for object recognition. In general, the above algorithms either have exponentially increased complexity as the number of candidate objects increases or have long feature vectors at each dyadic scale. Therefore, these techniques are not suitable for large databases with thousands of images.

In this paper, we propose an efficient biorthogonal-wavelet-transform-based approach to describe the contour features of a given object. The remainder is organized as follows: Section 2 proposes our object contour matching algorithm. Section 3 illustrates the experimental results. Section 4 draws conclusions.

## 2. Object Contour Matching Method

This section details the step-by-step procedure to match object contours. We focus on a boundary-based representation of object contours rather than a region-based one due to lateral inhibition, which behaves like the high-pass Laplacian operator [3]. Therefore, our digital image data exclusively contains one non-occluded object boundary per image.

### 2.1 Preprocess each query and candidate image

A preprocessing step is necessary to pad the boundaries of any image with an odd number of rows or columns since an integer wavelet transform requires the number of rows and columns to be even.

### 2.2 Apply a one-level biorthogonal wavelet transform to each preprocessed query and candidate image

- The choice of a wavelet transform

To date, we have used the (2, 2) integer wavelet transform (IWT). It is a family of symmetric, biorthogonal wavelet transforms constructed from the

interpolating Deslauriers-Dubuc scaling functions [8]. Different sets of  $(N_1, N_2)$  can be used to conduct both forward and inverse IWTs, where  $N_1$  and  $N_2$  respectively represent the number of vanishing moments of the analyzing high-pass filter and the synthesizing high-pass filter. The (2, 2) IWT is repetitively constructed by:

$$\begin{aligned} d_{i,l} &= s_{i-1,2l+1} - \lfloor 1/2(s_{i-1,2l} + s_{i-1,2l+2}) + 1/2 \rfloor \\ s_{i,l} &= s_{i-1,2l} + \lfloor 1/4(d_{i,l-1} + d_{i,l}) + 1/2 \rfloor \end{aligned} \quad (1)$$

where  $s$  represents the original data sequence and  $l$  is the length (sample numbers) of the split sequences (i.e.,  $l$  is half of the length of the  $s$ ).

The reasons to choose (2, 2) IWT follow [9]: First, biorthogonal wavelet bases maintain the symmetry for wavelets and scaling functions by relaxing the orthogonality constraint and associating with short length filters. Second, the interpolating wavelet transforms are equally as amenable to most applications as orthogonal wavelet transforms. Third, keeping vanishing moments equally distributed for the analyzing and synthesizing high-pass filter obtains exactly symmetric biorthogonal wavelet systems.

- The choice of the wavelet decomposition level

In general, level two and three of the wavelet representation may be preferable for contour identifying, whereas the representation at level one is too sensitive to noise and representations at levels above four are too coarse for sensitivity to small changes. Since our image contains non-occluded object boundaries with little or no noise involved, we choose the level one decomposition. Such decomposition has the finest scale for fast computations as well as the least memory requirements.

### 2.3 Construct a wavelet transform modulus maxima (WTMM) image for each query and candidate image

Combine the low-high and high-low subbands from the multi-resolution representation of the image. These two subbands correspond to the object contour at the vertical and horizontal directions with the highest frequencies [10]. That is, each value in the WTMM image is calculated by  $\sqrt{LHValue^2 + HLValue^2}$ , where  $LHValue$  and  $HLValue$  are the values from the low-high and high-low subbands after level one wavelet transform.

### 2.4 Set up a threshold to determine the most important modulus maxima points (i.e., HCPs) for each query and candidate image

The threshold is empirically determined by:

$$Threshold = \begin{cases} Max/4 + Std & \text{if } \alpha > 0.04 \\ Max/2 + Std & \text{otherwise} \end{cases} \quad (2)$$

where  $\alpha$  is the amount (i.e., percentage) of the contour presented in an image,  $Max$  and  $Std$  are the maximum value and the standard deviation of the WTMM image. Any point with a value greater than  $Threshold$  corresponds to sharper edges (salient features) in the original image. Therefore, such a point is considered as a HCP in the WTMM image and kept for further processing.

### 2.5 Up-sample the WTMM image containing all HCPs to the original image size

### 2.6 Find the object centroid by averaging the coordinates of all HCPs

### 2.7 Construct a feature vector containing the sorted distances from each HCP to the centroid

If two feature vectors contain comparable values, the object contours represented by these two feature vectors are identical.

## 3. Experimental Results

We have divided the experimental images into two groups. The first group is formed by geometrical drawn objects that change their location, size, and angle in an image. The second group consists of fish contour images [11].

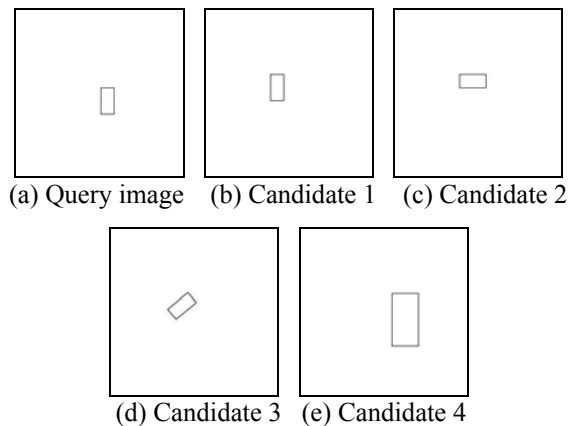
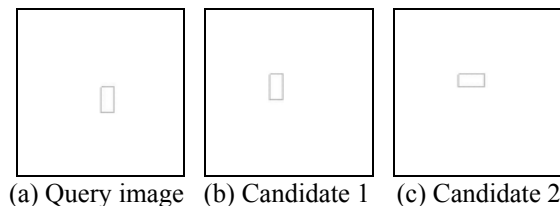
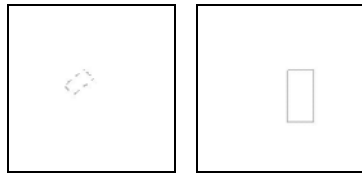


Figure 1: Rectangular objects in the first group

On Figure 1, the query image contains an object with a rectangular contour. All the four candidate images contain an object with the same rectangular contour but either being located at different positions, or being rotated by 90° or 40°, or being scaled by a factor of 2. The calculated WTMM images with the HCPs are illustrated on Figure 2.





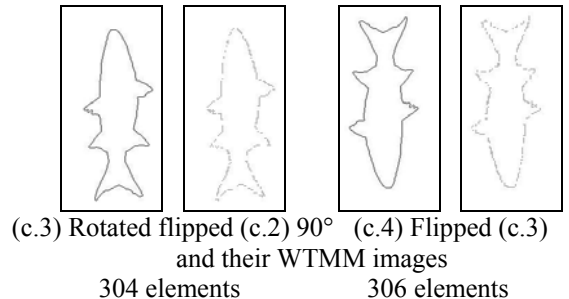
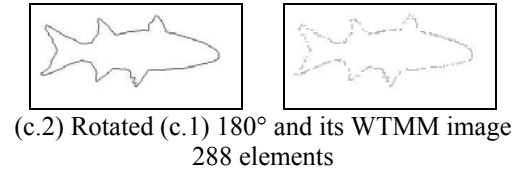
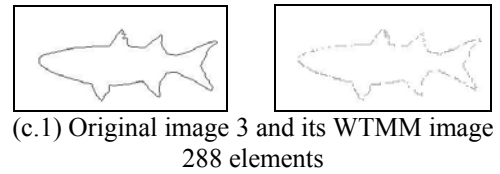
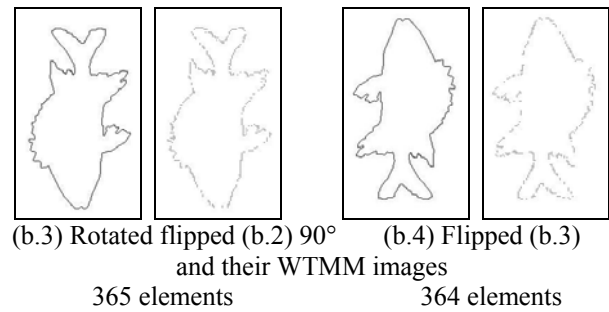
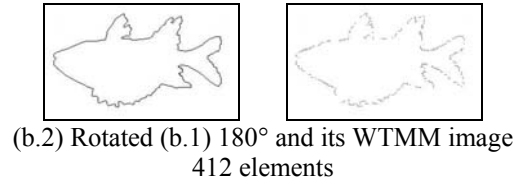
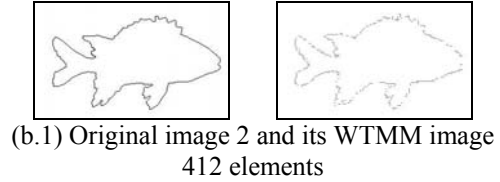
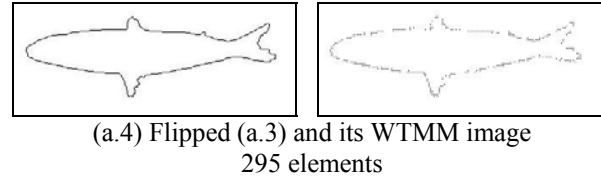
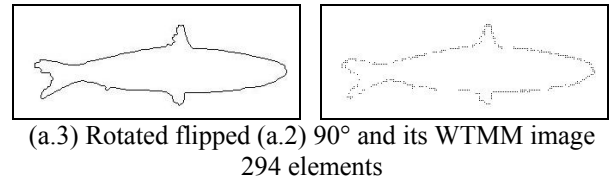
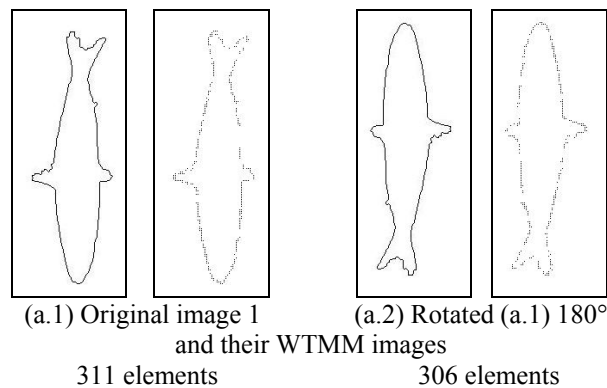
(d) Candidate 3 (e) Candidate 4  
Figure 2: WTMM images with the HCPs

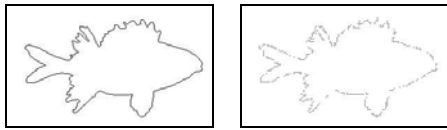
The feature vectors for the query image and the first two candidate images contain the following 59 elements:

9.0554, 9.0554, 9.4868, 9.4868, 10.2956,  
10.2956, 11.0454, 11.0454, 11.4018, 11.4018,  
11.4018, 11.4018, 12.0830, 12.0830, 12.7279,  
12.7279, 13.0384, 13.0384, 14.2127, 14.2127,  
14.2127, 14.2127, 15.5563, 15.5563, 15.8114,  
15.8114, 17.0294, 17.0294, 17.4929, 17.4929,  
18.6011, 18.6011, 19.0263, 19.0263, 19.2354,  
19.2354, 19.2354, 19.2354, 19.6469, 19.6469,  
20.2485, 20.2485, 20.2485, 20.2485, 21.0238,  
21.0238, 21.0238, 21.0238, 21.0238, 21.2132,  
21.2132, 21.5870, 21.5870, 21.9545, 21.9545,  
22.1359, 22.1359, 22.8473, 22.8473

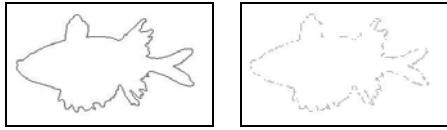
The feature vector for the fourth candidate contains 118 elements. Each paired adjacent element has the same values, which approximately double each corresponding value in the above feature vector. Such a similar pattern holds for different scaling factors. However, the feature vector for the third candidate contains 33 elements between 9.8489 and 23.7697, whose range is similar to the range of the above feature vector. The experimental results from the first group demonstrate our proposed feature vector is invariant to the changes in the translation, scale, and rotation.

Figure 3 shows several images from the second group. These images include the original images from the fish contour image database [11] and the corresponding rotated and flipped images. The WTMM images with the HCPs obtained by our proposed approach are illustrated at the right side of the corresponding original images. The feature vector size (i.e., the number of elements of the feature vector) is listed below each pair.

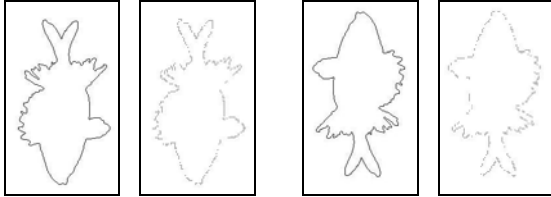




(d.1) Original image 4 and its WTMM image  
400 elements



(d.2) Rotated (d.1) 180° and its WTMM image  
398 elements



(d.3) Rotated flipped (d.2) 90° 326 elements  
(d.4) Flipped (d.3) 326 elements

Figure 3: Test images and WTMM images  
with the HCPs

The criteria to match two object contours are:

- 1) If two feature vectors have the same size and each element is close to the counterpart element with the difference of less than 0.5, the two object contours match.
- 2) If two feature vectors have size difference of either less than 80 for  $\alpha > 4\%$  ( $\alpha$  is the amount of the contour presented in an image) or less than 20 for  $\alpha \leq 4\%$ , group each element and its following elements when their values differ by less than 1. The average value of each group is sequentially utilized to construct a modified feature vector. If each element of the modified feature vector differs to its counterpart by a value of less than 0.5, the two object contours match.
- 3) If these two criteria failed, calculate a scaling factor as the ratio between two feature vector sizes. Approximately compare each element with its counterpart element by using the scaling factor in accordance with the repeated pattern explained in the first testing group. If such a repeated pattern exists, the two object contours with different size match.

The experimental results from the second group indicate the proposed approach can precisely match flipped object contours. For two identical object contours with different rotations or different sizes, our approach can adaptively match them by using the second or third criterion. As demonstrated by our experimental results, the accuracy for these two matches is high as well.

## 4. Conclusions

We propose a fast and robust matching algorithm for contour images by using a biorthogonal (2, 2) integer wavelet transform. The derived WTMM image contains only the HCPs, which represent the most salient features in the contour. A feature vector is constructed by the sorted distance between each HCP and the centroid of contour. This technique is invariant to the translation, rotation, and scale changes. It is very efficient to match the images within a large database due to the easy construction of the feature vector at only one dyadic scale of a wavelet transform.

## 5. Acknowledgement

Author acknowledges professors S. Abbasi, F. Mokhtarian, and J. Kittler for providing the test image databases.

## References

- [1] D. D. Hoffman, and W. A. Richards, "Parts of recognition," *Cognition*, Vol. 18, pp. 65-96, 1984.
- [2] C. H. Teh and R. T. Chin, "On the detection of dominant points on digital curves," *IEEE Trans. on PAMI*, vol. 11, pp. 859-872, 1989.
- [3] J. C. Russ, *The Image Processing Handbook*, 3rd edition, CRC, Springer and IEEE Press Inc., 1995.
- [4] M. H. Han and D. Jiang, "The use of maximum curvature points for the recognition of partially occluded objects," *Pattern Recognition*, Vol. 23, pp. 21-23, 1990.
- [5] F. A. Cheikh, A. Quddus, and M. Gabbouj, "Multi-level shape recognition based on wavelet-transform modulus maxima," *Proc. of Image Analysis and Interpretation*, pp. 8-12, April 2-4, 2000.
- [6] M. Khalil and M. Bayoumi, "Affine invariants for object recognition using the wavelet transform," *Pattern Recognition Letters*, Vol. 23, Issue1-3, pp. 57-72, 2002.
- [7] S. Belongie, J. Malik, and J. Puzicha, "Shape matching and object recognition using shape contexts," *IEEE Trans. on PAMI*, Vol. 24, No. 24, pp. 509-522, 2002.
- [8] W. Sweldens, "The lifting scheme: a custom-designed construction of biorthogonal wavelets," *Journal of Applied and Computational Harmonic Analysis*, pp. 186-200, 1996.
- [9] D. Wei, J. Tian, R. O. Wells, C. S. Burrus, "A new class of biorthogonal wavelet systems for image transform coding," *IEEE Trans. on Medical Imaging*, Vol. 7, No. 7, pp. 1000 - 1013, 1998.
- [10] S. Mallat and W. L. Hwang, "Singularity detection and processing with wavelets," *IEEE Trans. on Info. Theory*, Vol. 38, No. 2, March 1992.
- [11] Fish contour images, <http://www.ee.surrey.ac.uk/Research/VSSP/imagedb/de mo.html>